Crystalline structure of $SrAlF_5$ investigated by vibrational spectroscopy

2004 J. Phys.: Condens. Matter 16 7511

(http://iopscience.iop.org/0953-8984/16/41/028)

INSTITUTE OF PHYSICS PUBLISHING JOURNAL OF PHYSICS: CONDENSED MATTER

J. Phys.: Condens. Matter **16** (2004) 7511–7520 PII: S0953-8984(04)84379-0

Crystalline structure of $SrAlF_5$ investigated by vibrational spectroscopy

E N Silva[1], A P Ayala[1], J Mendes Filho[1], R L Moreira[2] and J-Y Gesland[3]

[1] Departamento de Física, Universidade Federal do Ceará, Caixa Postal 6030, 60451-900, Fortaleza, Ceará, Brazil
[2] Departamento de Física, ICEx, Universidade Federal de Minas Gerais, Caixa Postal 702, 30123-970, Belo Horizonte, (MG), Brazil
[3] Université du Maine—Cristallogénèse, UMR 6087, 72085 Le Mans Cedex 9, France

E-mail: ayala@fisica.ufc.br

Received 29 July 2004
Published 1 October 2004
Online at stacks.iop.org/JPhysCM/16/7511
doi:10.1088/0953-8984/16/41/028

Abstract

$SrAlF_5$ has been considered as one of the rare fluoride ferroelectric crystals, belonging to the polar $I4$ group. However, recent x-ray diffraction data suggest that the correct structure is centrosymmetric ($I4_1/a$). Since ferroelectricity is forbidden in this structure, the existence of an inversion centre was investigated by vibrational spectroscopy. Thus, measurements on $SrAlF_5$ single crystals have been made by polarized Raman scattering and infrared reflectance spectroscopy. The results, discussed on the basis of the factor group analysis of the proposed structures and other members of the ABF_5 family, favour a centrosymmetric structure.

1. Introduction

Ferroelectric materials are always subject of intensive research due to the large number of technological applications involving them. Despite the fact that most of the ferroelectric compounds are oxides, this property has been observed in a reduced set of fluoride materials. According to Ravez and Abrahams [1–3], ferroelectric fluorides belong to six families, namely $(NH_4)_2BeF_4$, $BaMnF_4$, $SrAlF_5$, Na_2MgAlF_7, $K_3Fe_5F_{15}$ and $Pb_3Cr_3F_{19}$. The origin of the spontaneous polarization in most of these families was described using the Abrahams–Kurtz–Jamieson (AKJ) theory [4], which correlates the Curie temperature with the atomic displacements between the paraelectric and ferroelectric crystalline structures.

In the special case of the $MAlF_5$ (M = Sr, Ca, Ba) family, Abrahams *et al* [5, 6], on the basis of the crystalline structure reported by von der Mühll *et al* [7], applied the AKJ

theory to predict a ferroelectric phase transition at 685 K in $SrAlF_5$. These authors confirmed the existence of a phase transition by observing anomalies in the dielectric constant and specific heat of polycrystalline samples at about 715 K. Supporting these results, Canouet *et al* [8] have also observed a phase transition at the same temperature in the crystal optical birefringence.

The interest in $SrAlF_5$ is not limited to its ferroelectric properties. Several authors have reported on its optical properties when used as a host for rare earth and transition metals. Cr^{3+} and Ce^{3+} doped $SrAlF_5$ exhibit wide emission bands [9–11], which are suitable for use in building solid-state tunable lasers. In order to improve the optical and spectroscopic characterization of the doped crystals, $SrAlF_5(Cr^{3+})$ crystals were investigated by electron paramagnetic resonance [12] and time resolved Z-scan and thermal lens techniques [13]. On the other hand, the emission spectra of Pr^{3+} doped crystals were also recorded, allowing the observation of photon cascade emission processes [14, 15]. Since alkaline earth sites are suitable for doping with divalent active ions [16–18], $SrAlF_5$ offers the possibility of co-doping the crystal with a active ions emitting in the visible and UV spectral region, as was shown by van der Kolk *et al* [19].

Despite the experimental evidence supporting the existence of a high temperature phase transition in $SrAlF_5$, there have been no results published reporting direct evidence of the ferroelectric character of this material. Similarly to other fluoride compounds, $SrAlF_5$ exhibits a high ionic conductivity at high temperatures. This feature makes it difficult to perform polarization loops or to polarize the crystal. Recently, Kubel [20] presented a single-crystal x-ray diffraction study of $SrAlF_5$. According to these results, the $SrAlF_5$ structure would be tetragonal, belonging to the $I4_1/a$ space group. However, the presence of an inversion centre in the $I4_1/a$ space group forbids ferroelectricity in such a compound. Thus, considering the discrepancy between the structural and theoretical results, the aim of this work is to investigate the existence of an inversion centre in $SrAlF_5$ by using polarized Raman and infrared spectroscopies.

2. Experimental procedures

Due to the technological interest, several methods of synthesis for obtaining $SrAlF_5$ have been tested. $SrAlF_5$ melts congruently at 887 °C [18, 21–24]. As raw materials, SrF_2 single-crystalline pieces and AlF_3, synthesized by fluorination of pure alumina with NH_4HF_2 and separated from NH_4F by pyrolysis, were used. Single crystals of $SrAlF_5$ were grown from stoichiometric melt, in an argon–CF_4–HF mixed atmosphere by the Bridgman method, in well-closed graphite crucibles. The temperature gradient was approximately 20 °C cm^{-1} and the translation speed was 1 mm h^{-1}.

Reflection infrared spectra were recorded with a Bomem DA8 Fourier transform spectrometer, in the wavenumber range from 25 to 4000 cm^{-1}. The spectral resolution was typically 4 cm^{-1}. For the mid-infrared region (above 500 cm^{-1}), the best choice of accessories was: a Globar source, a KBr beam splitter, a ZnSe polarizer and a LN_2-cooled HgCdTe detector. The far infrared region was measured using a Globar or a mercury arc lamp (below 200 cm^{-1}), a 6 μm Mylar coated Hypersplitter^{TM}, a polyethylene polarizer and a LHe-cooled Si bolometer.

Raman spectra were recorded by using a Jobin-Yvon Triplemate Spectrometer (model T64000) equipped with a LN_2-cooled CCD detector. The spectra were recorded in the backscattering configuration, using 50 mW of the 514.5 nm line of an argon ion laser as the exciting source. Scattering geometries for the Raman spectra listed in the text and figures follow the usual Porto notation, $A(BC)D$ [25].

Table 1. Vibrational selection rules of the C_4 and C_{4h} point groups.

	C_4	C_{4h}
	Raman scattering	
$z(xx)\bar{z}$	A(LO) ⊕ B	$A_g \oplus B_g$
$y(xx)\bar{y}$	A(TO) ⊕ B	$A_g \oplus B_g$
$z(xy)\bar{z}$	B	B_g
$y(zz)\bar{y}$	A(TO)	A_g
$y(zx)\bar{y}$	E(TO) ⊕ E(LO)	E_g
	Infrared reflectance	
$E \parallel z$	A	A_u
$E \perp z$	E	E_u

3. Group theory

As is well known, Raman and infrared spectroscopies allow one to obtain the optical phonon spectra of crystals. However, these techniques are generally complementary and only in few cases of polar structures do they give individually the same phonon modes. On the other hand, in the case of the ten centrosymmetric point groups, the mutual exclusion principle claims that not all the infrared-active irreducible representations (ir) can be Raman active, and vice versa. On the basis of the symmetry transformation rules of linear and quadratic base functions, one can then use infrared and Raman techniques to identify the presence of an inversion centre in a crystalline structure.

The first $SrAlF_5$ crystalline structure was determined by von der Mühll *et al* [7]; they proposed a body centred tetragonal lattice belonging to the I_4 (C_4^5) space group, with 16 molecules per unit cell. In this structure, the fluorine anions are distributed in two 2a, one 4b and nine 8c crystalline sites. Aluminium cations occupy two 2a, one 4b and one 8c site, whereas strontiums are at two 8b sites. Using the site group method proposed by Rousseau *et al* [26], we obtain the following distribution of the degrees of freedom in terms of the ir of the C_4 point group:

$$\Gamma = 42\mathrm{A} \oplus 38\mathrm{B} \oplus 44\mathrm{E}. \tag{1}$$

According to the character table of the C_4 point group, all ir are Raman active. Moreover, A and E representations are also infrared active, with polarizations lying along the z-axis and in the xy-plane, respectively. Furthermore, polar modes (A and E) split in transverse ($\tilde{\nu}_{TO}$) and longitudinal ($\tilde{\nu}_{LO}$) modes, which are observed together in the infrared spectra but may be selected in a polarized Raman experiment. Thus, the Raman-active ir in different Raman scattering geometries and infrared ir with the electrical field polarized along and perpendicularly to the z-direction of the crystal are listed in table 1, besides those of the C_{4h} group discussed below.

The $SrAlF_5$ structure reported by Kubel [20] is also tetragonal body centred, but belongs to the $I4_1/a$ space group with 64 molecules per unit cell. Fluorine ions are distributed in twenty 16f sites, strontium in four 16f sites and aluminium occupies three 16f and two 8e crystallographic sites. This atomic distribution gives rise to the following irreducible representation at the centre of the Brillouin zone:

$$\Gamma = 83\mathrm{A_g} \oplus 82\mathrm{A_u} \oplus 83\mathrm{B_g} \oplus 83\mathrm{B_u} \oplus 85\mathrm{E_g} \oplus 84\mathrm{E_u}, \tag{2}$$

where *gerade* A_g, B_g and E_g representations are Raman active and the *ungerade* A_u and E_u representations are infrared active. B_u type phonons are active neither in Raman nor in infrared

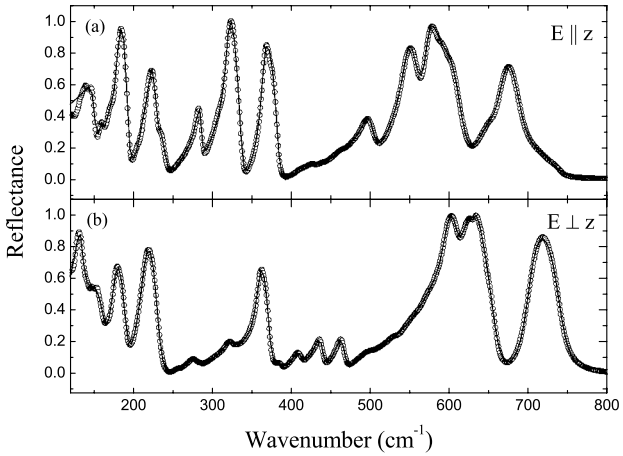

Figure 1. Infrared reflectivity of $SrAlF_5$ single crystals recorded with the electric field (a) parallel and (b) perpendicular to the z-axis.

spectroscopies and are known as *silent modes*. The optically active ir of the C_{4h} group in the different measuring configurations are shown in table 1.

4. Results

4.1. Infrared reflectance

Infrared reflectance spectra recorded by using electromagnetic radiation polarized parallel ($E \parallel z$) and perpendicular ($E \perp z$) to the principal axis of the $SrAlF_5$ structure are shown in figure 1. These results were analysed by using the four-parameter semi-quantum model [27]. According to this model, the complex dielectric constant is expressed in terms of the infrared-active modes as follows:

$$\varepsilon(\omega) = \varepsilon_\infty \prod_j \frac{\omega_{j\mathrm{LO}}^2 - \omega^2 + \mathrm{i}\omega\gamma_{j\mathrm{LO}}}{\omega_{j\mathrm{TO}}^2 - \omega^2 + \mathrm{i}\omega\gamma_{j\mathrm{TO}}}, \tag{3}$$

where $\omega_{j\mathrm{TO}}$ and $\omega_{j\mathrm{LO}}$ correspond to the resonance frequencies of the jth transverse and longitudinal modes, respectively, and $\gamma_{j\mathrm{TO}}$ and $\gamma_{j\mathrm{LO}}$ are the corresponding damping factors. ε_∞ is the dielectric constant due to the electronic polarization. The observed infrared reflectivity R is fitted with the aid of equation (3), together with

$$R = \left| \frac{\sqrt{\varepsilon} - 1}{\sqrt{\varepsilon} + 1} \right|^2. \tag{4}$$

From the best fit of the experimental data using equations (3) and (4) we obtained the wavenumbers of the transverse (TO) and longitudinal (LO) infrared-active modes, which are listed in table 2, for both the $E \parallel z$ and $E \perp z$ polarizations. The number of observed bands is lower than that predicted by group theory for the two proposed structures. It is interesting to note that it corresponds approximately to one half and one quarter of the expected number of modes for the C_4 and C_{4h} structures, respectively. We will discuss this behaviour in more detail later.

Once the infrared-active vibrational modes are determined, the oscillator strengths $\Delta\varepsilon_j$ of the jth transverse modes can be directly deduced from the LO/TO splitting, through the

Table 2. Vibrational modes (in cm^{-1}) of $SrAlF_5$, assuming a C_{4h} point group symmetry. For the *ungerade* species A_u and E_u, transverse (TO) e longitudinal (LO) modes are separated by slashes.

A_g	B_g	E_g	A_u	E_u
96	139	32	146/153	131/136
100	147	98	159/160	155/165
215	149	107	182/194	177/192
247	160	136	220/230	212/233
260	165	154	235/240	275/276
340	171	154	283/286	276/278
369	219	178	319/337	322/324
393	231	191	365/378	359/361
404	290	201	379/382	363/373
431	330	209	434/436	377/386
459	363	216	440/441	408/411
515	374	239	497/504	436/440
527	399	293	547/563	463/468
547	448	345	570/572	496/498
600	491	391	610/616	573/580
626	733	422	645/646	596/611
676		690	666/685	616/631
			730/738	631/657
				700/740

relation

$$\Delta\varepsilon_j = \frac{\varepsilon_\infty}{\omega_{j\mathrm{TO}}^2} \times \frac{\prod_k (\omega_{k\mathrm{LO}}^2 - \omega_{j\mathrm{TO}}^2)}{\prod_{k\neq j} (\omega_{k\mathrm{TO}}^2 - \omega_{j\mathrm{TO}}^2)}. \tag{5}$$

Furthermore, the static dielectric constant can be obtained by adding the strengths of all oscillators, that is

$$\varepsilon_\mathrm{s} = \varepsilon_\infty + \sum_j \Delta\varepsilon_j. \tag{6}$$

The high frequency dielectric constant obtained from the fit where $\varepsilon_\infty^\perp = 2.25$ and $\varepsilon_\infty^\parallel = 2.36$, which correspond to a refraction index of ∼1.5, is in good agreement with the previously reported values from optical measurements [28]. By using equation (6), we obtained the main components of the static dielectric constant tensor; that is, by adding the oscillator strengths ($\Delta\varepsilon_j$) the following low frequency dielectric constant were calculated: $\varepsilon_\mathrm{s}^\perp = 6.57$ and $\varepsilon_\mathrm{s}^\parallel = 5.14$. These values agree very well with those of impedance spectroscopy measurements recorded at 100 kHz, $\varepsilon^\perp = 8.45$ and $\varepsilon^\parallel = 7.75$ [29]. These values are slightly higher than the infrared ones; the difference probably originates from the contribution of low energy phonons ($\tilde{\nu} < 130\ cm^{-1}$) that were not observed in our results. The existence of such phonons is supported by the Raman scattering results presented in the next section. The proximity of the dielectric constant values in the radio-frequency and optical spectral ranges results from the absence of polar domains and dipoles, since the main contribution to the static dielectric constant arises from the polar phonons. This observation favours the centrosymmetric structure over the polar one.

4.2. Raman scattering

Raman spectra were recorded in several scattering geometries available in a backscattering configuration. In figure 2 we plotted the spectra corresponding to the excitation of the xx,

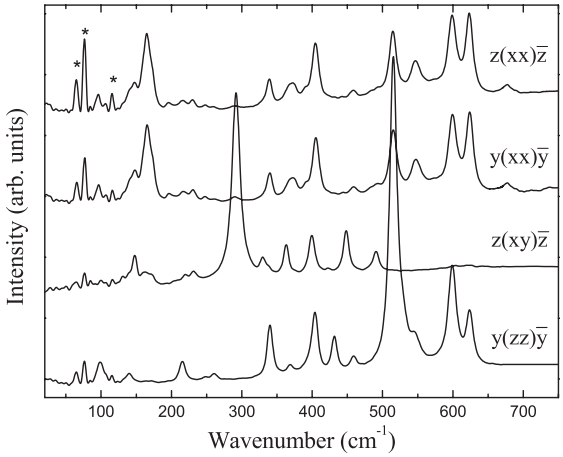

Figure 2. Raman spectra recorded in the $z(xx)\bar{z}$, $y(xx)\bar{y}$, $z(xy)\bar{z}$ and $y(zz)\bar{y}$ scattering geometries. Asterisks indicate spurious lines due to laser plasma emissions.

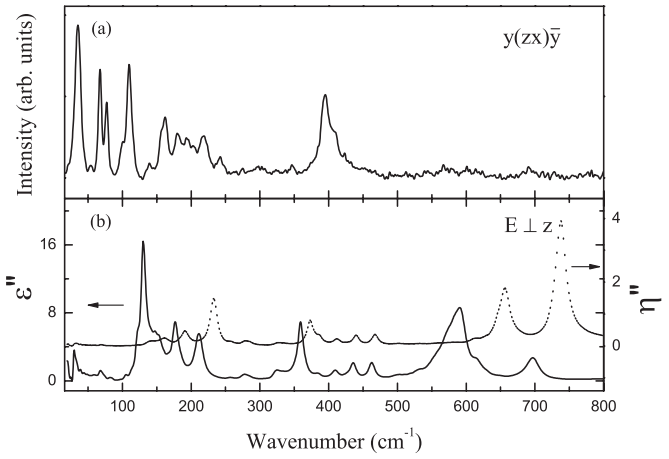

Figure 3. Comparison between (a) Raman spectra and (b) infrared dielectric functions related to E (or E_g and E_u) modes.

xy and zz components of the polarizability tensor. According to table 1, the A (A_g) and B (B_g) irs of the C_4 (C_{4h}) point group should be observed in these spectra. On the other hand, the bi-dimensional representations (E or E_g) are active in the $y(xz)\bar{y}$ scattering geometries, as shown in figure 3(a). All of these spectra were analysed by fitting them to a set of damped harmonic oscillators. The wavenumbers of the oscillators which produced the best fit of the experimental data are listed in table 2. Notice that 17, 16 and 17 modes can be associated with the A (A_g), B (B_g) and E (E_g) irs of the C_4 (C_{4h}) point group. As in the case of the infrared spectra, about one half (one quarter) of the predicted modes for the C_4 (C_{4h}) point group were observed.

5. Discussion

As was pointed out, there is a discrepancy between the ferroelectric character of $SrAlF_5$ and the recently reported crystalline structure, which is centrosymmetric, because the presence of an

inversion centre forbids ferroelectricity [30]. There are several methods for checking whether a compound is centrosymmetric. The commonest is that based on second-harmonic generation (SHG). In fact, Abrahams *et al* claimed that this effect was observed for polycrystalline $SrAlF_5$ [5]. However, several attempts to observe SHG in large $SrAlF_5$ single crystals by our group were unsuccessful. Furthermore, neither electro-optical modulation nor piezoelectric experiments give results supporting the absence of an inversion centre in $SrAlF_5$ [29]. Thus, the SHG observed in polycrystalline $SrAlF_5$ could be a non-intrinsic effect, since small particles of a centrosymmetric compound, such as those of a polycrystalline sample, may exhibit this property due to the suppression of the inversion symmetry at the surface [31].

Since the conventional techniques fail to demonstrate the absence of an inversion centre in $SrAlF_5$, some insight into this problem can be obtained by using polarized optical spectroscopies. The sensitivity of these techniques for defining the polar character of a crystal is given by the vibrational selection rules. Thus, in a centrosymmetric system Raman-active phonons are forbidden to be infrared active and vice versa. Conversely, in a polar crystal, phonons belonging to some irreducible representations may be observed by both techniques. Furthermore, for Raman-active polar phonons the transverse or longitudinal components may be recorded separately with an appropriate choice of the scattering geometry. We used these properties to shed some light on the problem of the $SrAlF_5$ ferroelectricity.

First, consider the polarized Raman spectra plotted in figure 2. According to table 1, depending on the scattering geometry, symmetric (A or A_g) or anti-symmetric (B or B_g) representations with respect to the main axis are Raman active. In the case of the C_4 polar system, transverse (A(TO)) and longitudinal (A(LO)) components of the A polar representation should be observed, respectively, in the $y(xx)\bar{y}$ and $z(xx)\bar{z}$ scattering geometries. Due to the Lyddane–Suchs–Teller relationship [27], the energy of the transverse modes must be lower than that of the longitudinal ones. Thus, if A modes are present in the $y(xx)\bar{y}$ and $z(xx)\bar{z}$ spectra, differences between them should be observed not only in the energy of the modes but also in their relative intensities. However, figure 2 shows that these spectra are practically identical, as should be expected in the case where the crystal belongs to the C_{4h} point group, where non-polar A_g modes are predicted by group theory for both geometries (see table 1).

As was pointed out above, in a polar system some irreducible representation should be Raman and infrared active. That is the case for the A and E representations of the C_4 point group. Raman and infrared results can be better compared by calculating the imaginary parts of the complex dielectric constant ε'' and its inverse $\eta'' = \mathrm{Im}(1/\varepsilon)$. It is well known that ε'' and η'' exhibit peaks at the frequencies of the transverse and longitudinal optical modes, respectively. In view of this, in figure 4, $y(xx)\bar{y}$ and $y(zz)\bar{y}$ scattering geometries are compared with ε'' and η'' calculated from the results of the fit of the $E \parallel z$ infrared spectrum. On the other hand, in figure 3, the $y(zx)\bar{y}$ Raman spectrum is compared with the corresponding optical function obtained from the $E \perp z$ spectrum. According to table 1, A and E polar modes should be observed, respectively, in figures 3 and 4 if $SrAlF_5$ belongs to the $I4$ space group. As a consequence, TO and LO bands should be observed at the same energies in both Raman and infrared optical functions. However, we cannot establish any association between Raman and infrared bands, either in figure 3 or in figure 4. Conversely, these results agree with a non-polar point group, where *gerade* (A_g, B_g) and *ungerade* (A_u, E_u) should be observed separately in Raman and IR spectra, without an *a priori* correlation between their energies. Since this method was successfully applied to other fluoride crystals [32, 33] to verify their polar character, we note that our polarized vibrational spectra supported the existence of an inversion centre in $SrAlF_5$ and consequently the absence of ferroelectric nature of this material.

Finally, the origin of the small number of observed vibrational bands when compared with that predicted by the factor group analysis of the published crystalline structures needs

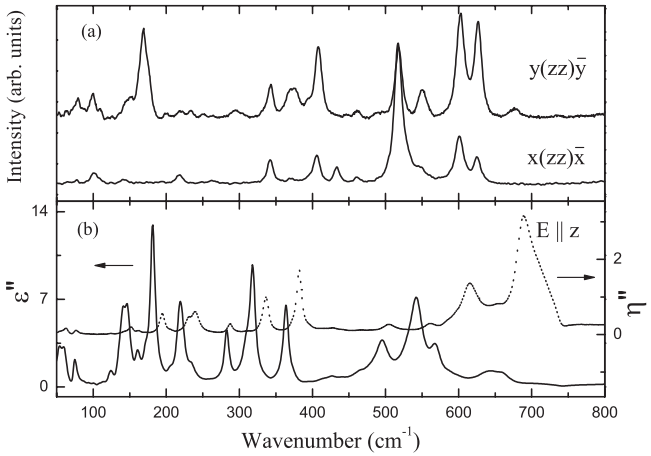

Figure 4. Comparison between (a) Raman spectra and (b) infrared dielectric functions related to A (or A_g and A_u) modes.

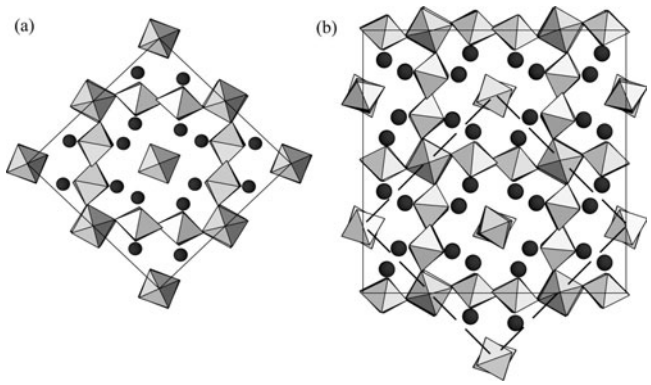

Figure 5. Projection of the (a) $I4$ and (b) $I4_1/a$ crystalline structures of $SrAlF_5$ along of the [001] direction of the crystal.

to be discussed. First, let us briefly compare the two structures, which are plotted in figure 5. Despite the increase of Z from 16 to 64 due to the enlarging of the unit cell, three families of different AlF_6 octahedra can be easily identified using as a reference the $I4$ structure: (i) the AlF_6 octahedra placed at the vertices and body centre; (ii) those at the middles of the edges; and (iii) those aligned parallel to the face diagonals. By comparing the two structures, one can easily notice that the main difference between them is related to the first family. Thus, these octahedra form chains aligned along the z-axis sharing the apical anions in the $I4$ structure. These chains are broken in the $I4_1/a$ structure, forming a dimer (Al_2F_{10}) of two octahedra parallel to the ab-plane sharing an edge.

In order to correlate the structure transformations with the vibrational spectra, one can introduce the new symmetry elements one by one. First, the horizontal mirror, which gives rise to the inversion centre, may be considered. The addition of this symmetry element transforms the space group into $I4/m$ ($Z = 16$), as was reported for $Ba_{0.433}Sr_{0.568}AlF_5$ [20], but the crystalline axes remain the same as in the $I4$ structure. Due to the group–subgroup relationship ($C_{4h} \rightarrow C_4$), one should expected the ir to be correlated according to: $A \rightarrow A_g + A_u$,

$B \rightarrow B_g + B_u$ and $E \rightarrow E_g + E_u$. As a consequence, approximately half of the vibrational bands predicted for the $I4$ structure become Raman active (A_g, B_g and E_g) and the remaining ones become infrared active (A_u and E_u) or silent (B_u). Such a transformation halves the number of expected modes in good agreement with our results.

Recently, Weil *et al* [34] reported a monoclinic modification of $SrAlF_5$. Since all of our results, including optical birefringence measurements [29], support the existence of a tetragonal axis, the monoclinic structure will not be considered in our discussion. Another group of centrosymmetric members of the ABF_5 family is formed by $BaTiF_5$ [35], $LiUF_5$ [36], $SmAlF_5$ [37] and $YbAlF_5$ [38]. These compounds also belong to the $I4/m$ space group with $Z = 16$, but the characteristic dimer of the $I4_1/a$ structure is tilted along the shared edge and disordered around the z-axis. By comparing $BaTiF_5$ and Kubel's structures one can note that they are related by transforming the symmorphic symmetry elements 4 and $/m$ into non-symmorphic ones, that is, a screw axis (4_1) and a glide plane ($/a$). As a consequence, the x-and y-axes are rotated by 45°, which, combined with the doubling of the c parameter, increases the number of molecules per unit cell from 16 to 64. Thus, the orientational disorder of the Al_2F_{10} dimers is suppressed; they become ordered and related by the screw axis. Due to this, Kubel's structure could be considered as an ordered superstructure of the $BaTiF_5$ one. If the two structures are related by small distortion, one could analyse the vibrational spectra of $SrAlF_5$ on the basis of a reduced cell ($Z = 16$) with $I4/m$ pseudo-symmetry. As was pointed out, such structure gives rise to a number of vibrational modes, which is in accord with the experimental observations. However, neither Raman scattering nor infrared reflectance could be used to distinguish between the ordered and disordered possible structures of $SrAlF_5$.

6. Conclusions

Polarized Raman scattering and infrared reflectance have been used to investigate the vibrational spectrum of $SrAlF_5$ single crystals. The results were analysed on the basis of the proposed crystalline structures. As a consequence, the phonon spectra were found to support the presence of an inversion centre in $SrAlF_5$, forbidding the existence of ferroelectricity in this material. The origin of the observation of a reduced number of vibrational modes was discussed by comparing the crystalline structures of several members of the ABF_5 family; this showed that the vibrational spectra may be associated with a tetragonal lattice with $Z = 16$ and $I4/m$ pseudo-symmetry.

Acknowledgments

This work was partially supported by the Brazilian government agencies CNPq, CAPES, FUNCAP and FAPEMIG.

References

[1] Abrahams S C and Ravez J 1992 *Ferroelectrics* **135** 21
[2] Ravez J 1997 *J. Physique* III **7** 1129
[3] Ravez J 2000 *C. R. Acad. Sci.* IIC **3** 267
[4] Abrahams S C, Kurtz S K and Jamieson P B 1968 *Phys. Rev.* **172** 551
[5] Abrahams S C, Ravez J, Simon A and Chaminade J P 1981 *J. Appl. Phys.* **52** 4740
[6] Ravez J, Abrahams S C, Chaminade J P, Simon A, Grannec J and Hagenmuller P 1981 *Ferroelectrics* **38** 773
[7] von der Mühll R, Andersson S and Galy J 1971 *Acta Crystallogr.* B **27** 2345
[8] Canouet S, Ravez J and Hagenmuller P 1985 *J. Fluorine Chem.* **27** 241
[9] Lai S T, Jenssen H P and Gabbe D 1985 *J. Opt. Soc. Am.* A **2** 44

[10] Jenssen H P and Lai S T 1986 *J. Opt. Soc. Am.* B **3** 115
[11] Dubinskii M A, Schepler K L, Semashko V V, Abdulsabirov R Y, Korableva S L and Naumov A K 1998 *J. Mod. Opt.* **45** 221
[12] Wang D M, Hutton D R, Troup G J and Jenssen H P 1986 *Phys. Status Solidi* a **98** K73
[13] Andrade A A, Tenorio E, Catunda T, Baesso M L, Cassanho A and Jenssen H P 1999 *J. Opt. Soc. Am.* B **16** 395
[14] Rodnyi P A, Mikhrin S B, Dorenbos P, van der Kolk E, van Eijk C W E, Vink A P and Avanesov A G 2002 *Opt. Commun.* **204** 237
[15] Vink A P, Dorenbos P, de Haas J T M, Donker H, Rodnyi P A, Avanesov A G and van Eijk C W E 2002 *J. Phys.: Condens. Matter* **14** 8889
[16] Hewes R A and Hoffman M V 1971 *J. Lumin.* **3** 261
[17] Hoffman M V 1971 *J. Electrochem. Soc.* **118** 933
[18] Meehan J P and Wilson E J 1972 *J. Cryst. Growth* **15** 141
[19] van der Kolk E, Dorenbos P, van Eijk C W E, Vink A P, Weil M and Chaminade J P 2004 *J. Appl. Phys.* **95** 7867
[20] Kubel F 1998 *Z. Anorg. Allg. Chem.* **624** 1481
[21] Fujihara S, Ono S, Kishiki Y, Tada M and Kimura T 2000 *J. Fluorine Chem.* **105** 65
[22] Weil M and Kubel F 2002 *J. Solid State Chem.* **164** 150
[23] Jia Z H, Hua R N and Shi C S 2003 *Chin. J. Chem.* **21** 1035
[24] Klimm D and Reiche P 2003 *J. Cryst. Growth* **249** 388
[25] Porto S P S and Scott J F 1967 *Phys. Rev.* **157** 716
[26] Rousseau D L, Bauman R P and Porto S P S 1981 *J. Raman Spectrosc.* **10** 253
[27] Gervais F and Echegut P 1986 *Incommensurete Phases in Dielectrics* ed R Blinc and A P Levanyuk (Amsterdam: North-Holland) p 337
[28] Deloach L D, Payne S A, Chase L L, Smith L K, Kway W L and Krupke W F 1993 *IEEE J. Quantum Electron.* **29** 1179
[29] Righi A and Moreira R L 2004 private communication
[30] Nye J F 1957 *Physical Properties of Crystal: their Representation by Tensor and Matrices* (Oxford: Clarendon)
[31] Dadap J I, Shan J, Eisenthal K B and Heinz T F 1999 *Phys. Rev. Lett.* **83** 4045
[32] Teixeira E, Mendes J, Melo F E, Ayala A P, Gesland J Y, Paschoal C W A and Moreira R L 2003 *Vib. Spectrosc.* **31** 159
[33] Ayala A P, Paschoal C W A, Gesland J Y, Ellena J, Castellano E E and Moreira R L 2002 *J. Phys.: Condens. Matter* **14** 5485
[34] Weil M, Zobetz E, Werner F and Kubel F 2001 *Solid State Sci.* **3** 441
[35] Eicher S M and Greedan J E 1984 *J. Phys.: Condens. Matter* **52** 12
[36] Brunton G 1966 *Acta Crystallogr.* **21** 12
[37] Koehler J 1993 *Z. Anorg. Allg. Chem.* **619** 181
[38] Koehler J 1999 *Solid State Sci.* **1** 545